

1 **Characterization of the light absorbing properties, chromophores composition**  
2 **and sources of brown carbon aerosol in Xi'an, Northwest China**

3 Wei Yuan<sup>1,2</sup>, Ru-Jin Huang<sup>1,3</sup>, Lu Yang<sup>1</sup>, Jie Guo<sup>1</sup>, Ziyi Chen<sup>4</sup>, Jing Duan<sup>1,2</sup>, Meng Wang<sup>1,2</sup>, Ting  
4 Wang<sup>1,2</sup>, Haiyan Ni<sup>1</sup>, Yongming Han<sup>1</sup>, Yongjie Li<sup>5</sup>, Qi Chen<sup>6</sup>, Yang Chen<sup>7</sup>, Thorsten Hoffmann<sup>8</sup>,  
5 Colin O'Dowd<sup>9</sup>

6 <sup>1</sup>State Key Laboratory of Loess and Quaternary Geology, Center for Excellence in Quaternary  
7 Science and Global Change, Chinese Academy of Sciences, and Key Laboratory of Aerosol  
8 Chemistry & Physics, Institute of Earth Environment, Chinese Academy of Sciences, Xi'an  
9 710061, China

10 <sup>2</sup>University of Chinese Academy of Sciences, Beijing 100049, China

11 <sup>3</sup>Institute of Global Environmental Change, Xi'an Jiaotong University, Xi'an 710049, China

12 <sup>4</sup>Royal School of Mines, South Kensington Campus, Imperial College London, Exhibition  
13 Road, London SW7 3RW, United Kingdom

14 <sup>5</sup>Department of Civil and Environmental Engineering, Faculty of Science and Technology,  
15 University of Macau, Taipa, Macau 999078, China

16 <sup>6</sup>State Key Joint Laboratory of Environmental Simulation and Pollution Control, College of  
17 Environmental Sciences and Engineering, Peking University, Beijing 100871, China

18 <sup>7</sup>Chongqing Institute of Green and Intelligent Technology, Chinese Academy of Sciences,  
19 Chongqing 400714, China

20 <sup>8</sup>Institute of Inorganic and Analytical Chemistry, Johannes Gutenberg University Mainz,  
21 Duesbergweg 10–14, Mainz 55128, Germany

22 <sup>9</sup>School of Physics and Centre for Climate and Air Pollution Studies, Ryan Institute, National  
23 University of Ireland Galway, University Road, Galway H91CF50, Ireland

24 *Correspondence to:* Ru-Jin Huang (rujin.huang@ieecas.cn)

25 **Abstract**

26 The impact of brown carbon aerosol (BrC) on the Earth's radiative forcing balance has

27 been widely recognized but remains uncertain, mainly because the relationships among BrC  
28 sources, chromophores, and optical properties of aerosol are poorly understood. In this work,  
29 the light absorption properties and chromophore composition of BrC were investigated for  
30 samples collected in Xi'an, Northwest China from 2015 to 2016. Both absorption Ångström  
31 exponent and mass absorption efficiency show distinct seasonal differences, which could be  
32 attributed to the differences in sources and chromophore composition of BrC. Three groups of  
33 light-absorbing organics were found to be important BrC chromophores, including compounds  
34 that have multiple absorption peaks at wavelength > 350 nm (12 polycyclic aromatic  
35 hydrocarbons and their derivatives) and compounds that have a single absorption peak at  
36 wavelength < 350 nm (10 nitrophenols and nitrosalicylic acids and 3 methoxyphenols). These  
37 measured BrC chromophores show distinct seasonal differences and contribute on average  
38 about 1.1% and 3.3% of light absorption of methanol-soluble BrC at 365 nm in summer and  
39 winter, respectively, about 7 and 5 times higher than the corresponding carbon mass fractions  
40 in total organic carbon. The sources of BrC were resolved by positive matrix factorization (PMF)  
41 using these chromophores instead of commonly used non-light absorbing organic markers as  
42 model inputs. Our results show that vehicular emissions and secondary formation are major  
43 sources of BrC (~70%) in spring, coal combustion and vehicular emissions are major sources  
44 (~70%) in fall, biomass burning and coal combustion become major sources (~80%) in winter,  
45 while secondary BrC dominates (~60%) in summer.

## 46 **1 Introduction**

47 Brown carbon (BrC) is an important component of atmospheric aerosol particles and has  
48 significant effects on radiative forcing and climate (Feng et al., 2013; Laskin et al., 2015; Zhang  
49 et al., 2017a). BrC can efficiently absorb solar radiation and reduce the photolysis rates of  
50 atmospheric radicals (Jacobsan, 1999; Li et al., 2011; Mok et al., 2016), which ultimately  
51 influences the atmospheric photochemistry process, the formation of secondary organic aerosol  
52 (SOA), and therefore the regional air quality (Mohr et al., 2013; Laskin et al., 2015; Moise et  
53 al., 2015). In addition, some components in BrC, such as nitrated aromatic compounds (NACs)  
54 (Teich et al., 2017; Wang et al., 2018) and polycyclic aromatic hydrocarbons (PAHs)  
55 (Samburova et al., 2016; Huang et al., 2018), have adverse effects on human health (Bandowe

56 et al., 2014; Shen et al., 2018). The significant effects of BrC on environment, climate, air  
57 quality and living things call for more studies to understand its chemical characteristics, sources  
58 and the links with optical properties.

59 Investigating the chemical composition of BrC at molecular level is necessary, because  
60 even small amounts of compounds can have a significant effect on the light absorption  
61 properties of BrC and profound atmospheric implication (Mohr et al., 2013; Zhang et al., 2013;  
62 Teich et al., 2017; Huang et al., 2018). A number of studies have investigated the BrC  
63 composition at molecular level (Mohr et al., 2013; Zhang et al., 2013; Chow et al., 2015;  
64 Samburova et al., 2016; Lin et al., 2016, 2017, 2018; Teich et al., 2017; Huang et al., 2018; Lu  
65 et al., 2019). For example, Zhang et al. (2013) measured 8 NACs in Los Angeles and found that  
66 they contributed about 4% of water-soluble BrC absorption at 365 nm. Huang et al. (2018)  
67 measured 18 PAHs and their derivatives in Xi'an and found that they accounted for on average  
68 ~1.7% of the overall absorption of methanol-soluble BrC. A state-of-the-art high performance  
69 liquid chromatography-photodiode array-high resolution mass spectrometry (HPLC-PDA-  
70 HRMS) was applied to investigate the elemental composition of BrC chromophores in biomass  
71 burning aerosol (Lin et al., 2016, 2017, 2018). Lin et al. (2016) reported that in biofuels burning  
72 samples (sawgrass, peat, ponderosa pine, and black spruce), about 40-60% of the bulk BrC  
73 absorption in the wavelength range of 300-500 nm may be attributed to 20 strong chromophores  
74 and in another study (Lin et al., 2017) they reported that nitroaromatic compounds accounted  
75 for ~50% of the total absorption of water-soluble BrC during the biomass burning event in a  
76 nationwide bonfire festival in Israel. Despite these efforts, the molecular composition of  
77 atmospheric BrC still remains largely unknown due to its complexity in emission sources and  
78 formation processes.

79 Field observations and laboratory studies show that BrC has various sources, including  
80 primary emissions such as combustion and secondary formation from various atmospheric  
81 processes (Laskin et al., 2015). Biomass burning, including forest fires and burning of crop  
82 residues, is considered as the main source of BrC (Teich et al., 2017; Lin et al., 2017). Coal  
83 burning and vehicle emissions are also important primary sources of BrC (Yan et al., 2017; Xie  
84 et al., 2017; Sun et al., 2017; Li et al., 2019; Song et al., 2019). Secondary BrC is produced

85 through multiple-phase reactions occurring in or between gas phase, particle phase, and cloud  
86 droplets. For example, nitrification of aromatic compounds (Harrison et al., 2005; Lu et al.,  
87 2011), oligomers of acid-catalyzed condensation of hydroxyl aldehyde (De Haan et al., 2009;  
88 Shapiro et al., 2009), and reaction of ammonia (NH<sub>3</sub>) or amino acids with carbonyls (De Haan  
89 et al., 2011; Nguyen et al., 2013; Flores et al., 2014) can all produce BrC. Condensed phase  
90 reactions and aqueous-phase reactions have also been found to be important formation  
91 pathways for secondary BrC in ambient air (Gilardoni et al., 2016). In addition, atmospheric  
92 aging processes can lead to either enhancement or bleaching of the BrC absorption (Lambe et  
93 al., 2013; Lee et al., 2014; Zhong and Jang, 2014), further challenging the characterization of  
94 BrC.

95 As the starting point of the Silk Road, Xi'an is an important inland city in northwestern  
96 China experiencing severe particulate air pollution, especially during heating period with  
97 enhanced coal combustion and biomass burning activities (Wang et al., 2016; Ni et al., 2018).  
98 In this study, we performed spectroscopic measurement and chemical analysis of PM<sub>2.5</sub> filter  
99 samples in Xi'an to investigate: 1) seasonal variations in the light absorption properties and  
100 chromophore composition of BrC, and their relationships; 2) sources of BrC in different seasons  
101 based on positive matrix factorization (PMF) model with light-absorbing organic markers as  
102 input species.

## 103 **2 Experimental**

### 104 **2.1 Aerosol sampling**

105 A total of 112 daily ambient PM<sub>2.5</sub> filter samples were collected on pre-baked (780 °C, 3  
106 h) quartz-fiber filters (20.3 × 25.4 cm, Whatman, QM-A, Clifton, NJ, USA) in November-  
107 December 2015, April-May, July, October-November 2016, representing winter, spring,  
108 summer and fall, respectively. Filter samples were collected using a Hi-Vol PM<sub>2.5</sub> air sampler  
109 (Tisch, Cleveland, OH) at a flow rate of 1.05 m<sup>3</sup> min<sup>-1</sup> on the roof (~10 m above ground level,  
110 34.22°N, 109.01°E) of the Institute of Earth Environment, Chinese Academy of Sciences,  
111 which was surrounded by residential areas without large industrial activities. After collection,  
112 the filter samples were wrapped in baked aluminum foils and stored in a freezer (-20 °C) until

113 further analysis.

## 114 2.2 Light absorption measurement

115 One punch of loaded filter (0.526 cm<sup>2</sup>) was taken from each sample and sonicated for 30  
116 minutes in 10 mL of ultrapure water (> 18.2 MΩ · cm) or methanol (HPLC grade, J. T. Baker,  
117 Phillipsburg, NJ, USA). The extracts were then filtered with a 0.45 μm PTFE pore syringe filter  
118 to remove insoluble materials. The light absorption spectra of water-soluble and methanol-  
119 soluble BrC were measured with an UV-Vis spectrophotometer (300-700 nm) equipped with a  
120 liquid waveguide capillary cell (LWCC-3100, World Precision Instrument, Sarasota, FL, USA)  
121 following the method by Hecobian et al. (2010). The measured absorption data can be converted  
122 to the absorption coefficient Abs<sub>λ</sub> (M m<sup>-1</sup>) by equation (1):

$$123 \quad \text{Abs}_\lambda = (A_\lambda - A_{700}) \frac{V_1}{V_a \times L} \times \ln(10) \quad (1)$$

124 where A<sub>700</sub> is the absorption at 700 nm, serving as a reference to account for baseline drift, V<sub>1</sub>  
125 is the volume of water or methanol that the filter was extracted into, V<sub>a</sub> is the volume of sampled  
126 air, L is the optical path length (0.94 m). A factor of ln(10) is used to convert the log base-10  
127 (recorded by UV-Vis spectrophotometer) to natural logarithm to provide base-e absorption  
128 coefficient. The absorption coefficient of water-soluble or methanol-soluble organics at 365 nm  
129 (Abs<sub>365</sub>) is used to represent water-soluble or methanol-soluble BrC absorption, respectively.

130 The mass absorption efficiency (MAE: m<sup>2</sup> gC<sup>-1</sup>) of BrC in the extracts can be calculated  
131 as:

$$132 \quad \text{MAE}_\lambda = \frac{\text{Abs}_\lambda}{M} \quad (2)$$

133 where M (μgC m<sup>-3</sup>) is the concentration of water-soluble organic carbon (WSOC) for water  
134 extracts or methanol-soluble organic carbon (MSOC) for methanol extracts. Note that organic  
135 carbon (OC) is often used to replace MSOC because direct measurement of MSOC is  
136 technically difficult and many studies have shown that most of OC (~ 90%) can be extracted  
137 by methanol (Chen and Bond, 2010; Cheng et al., 2016; Xie et al., 2019).

138 The wavelength-dependent light absorption of chromophores in solution, termed as  
139 absorption Ångström exponent (AAE), can be described as:

$$140 \quad \text{Abs}_\lambda = K \cdot \lambda^{-\text{AAE}} \quad (3)$$

141 where  $K$  is a constant related to the concentration of chromophores and AAE is calculated by  
142 linear regression of  $\log \text{Abs}_\lambda$  versus  $\log \lambda$  in the wavelength range of 300-410 nm.

### 143 **2.3 Chemical analysis**

144 OC was measured with a thermal/optical carbon analyzer (DRI, model 2001) following  
145 the IMPROVE-A protocol (Chow et al., 2011). WSOC was measured with a TOC/TN analyzer  
146 (TOC-L, Shimadzu, Japan) (Ho et al., 2015).

147 Organic compounds listed in Table S1 were analyzed with a gas chromatograph-mass  
148 spectrometer (GC-MS, Agilent Technologies, Santa Clara, CA, USA). Prior to the GC-MS  
149 analysis, the silylation derivatization was conducted using a routine method (e.g., Wang et al.,  
150 2016; Al-Naiema and stone, 2017). Briefly, a quarter of 47 mm filter sample was ultrasonically  
151 extracted with 2 mL of methanol for 15 minutes and repeated three times. The extracts were  
152 filtered with a 0.45  $\mu\text{m}$  PTFE syringe filter and then evaporated with a rotary evaporator to  $\sim$ 1  
153 mL and dried with a gentle stream of nitrogen. Then, 50  $\mu\text{L}$  of  $\text{N,O}$ -  
154 bis(trimethylsilyl)trifluoroacetamide (BSTFA-TMCS; Fluka Analytical 99%) and 10  $\mu\text{L}$  of  
155 pyridine were added. The mixture was heated for 3 h at 70  $^\circ\text{C}$  for silylation. After reaction, 140  
156  $\mu\text{L}$  of *n*-hexane were added to dilute the derivatives. Finally, 2  $\mu\text{L}$  aliquot of the derivatized  
157 extracts were introduced into the GC-MS, which was equipped with a DB-5MS column  
158 (Agilent Technologies, Santa Clara, CA, USA), electron impact (EI) ionization source (70 eV),  
159 and a GC inlet of 280  $^\circ\text{C}$ . The GC oven temperature was held at 50  $^\circ\text{C}$  for 2 min, ramped to 120  
160  $^\circ\text{C}$  at a rate of 15  $^\circ\text{C min}^{-1}$ , and finally reached 300  $^\circ\text{C}$  at a rate of 5  $^\circ\text{C min}^{-1}$  (held for 16 min).  
161 Note that the derivatization for NACs was conducted at 70  $^\circ\text{C}$  for 3 h which is slightly different  
162 from the protocol used in Al-Naiema and stone (2017), because symmetrical peak shapes and  
163 high intensities for NACs can also be obtained under this condition in our study (see Fig. S1).  
164 In our study, 4-nitrophenol-2,3,5,6-d4 was used as an internal standard to correct for potential  
165 loss for NACs quantification (Chow et al., 2015). For the quantification of other organic  
166 compounds, an external standard method was used through daily calibration with working  
167 standard solutions. Also, for every 10 samples, a procedural blank and a spiked sample (i.e.,  
168 ambient sample spiked with known amounts of standards) were measured to check the  
169 interferences and recoveries. The measured recoveries were 80-102% and the uncertainties

170 (RSDs) were < 10% for measured organic compounds.

## 171 **2.4 Source apportionment of BrC**

172 Source apportionment of methanol-soluble BrC was performed using positive matrix  
173 factorization (PMF) as implemented by the multilinear engine (ME-2; Paatero, 1997) via the  
174 Source Finder (SoFi) interface written in Igor Wavemetrics (Canonaco et al., 2013). Abs<sub>365,MSOC</sub>  
175 and those light-absorbing species including fluoranthene (FLU), pyrene (PYR), chrysene  
176 (CHR), benzo(a)anthracene (BaA), benzo(a)pyrene (BaP), benzo(b)fluoranthene (BbF),  
177 benzo(k)fluoranthene (BkF), indeno[1,2,3-cd]pyrene (IcdP), benzo(ghi)perylene (BghiP), 9,10-  
178 anthracenequinone (9,10AQ), benzanthrone (BEN), benzo[b]fluoren-11-one (BbF11O),  
179 vanillic acid, vanillin and syringyl acetone were used as model inputs, together with some  
180 commonly used markers, i.e., phthalic acid, hopanes (17 $\alpha$ (H),21 $\beta$ (H)-30-norhopane,  
181 17 $\alpha$ (H),21 $\beta$ (H)-hopane, 17 $\alpha$ (H),21 $\beta$ (H)-(22S)-homohopane, 17 $\alpha$ (H),21 $\beta$ (H)-(22R)-  
182 homohopane, referred to as HP1-HP4, respectively), picene, and levoglucosan. The input data  
183 include species concentrations and uncertainties. The LOD (limit of detection), calculated as  
184 three times of the standard deviation of the blank filters, were used to estimate species-specific  
185 uncertainties, following Liu et al. (2017). Furthermore, for a clear separation of sources profiles,  
186 the contribution of corresponding markers was set to 0 in the sources unrelated to the markers  
187 (see Table S2). This source apportionment protocol is very similar to our previous study (Huang  
188 et al., 2014).

## 189 **3 Results and discussion**

### 190 **3.1 Light absorption properties of water- and methanol-soluble BrC**

191 Fig. 1 shows the temporal profiles of Abs<sub>365</sub> of water- and methanol-soluble BrC, together  
192 with the concentrations of WSOC and OC (representing MSOC). They all show similar  
193 seasonal variations with the highest average in winter, followed by fall, spring and summer (see  
194 Table S3). WSOC contributed annually  $54.4 \pm 16.2\%$  of the OC mass, with the highest  
195 contribution in summer ( $66.1 \pm 15.5\%$ ) and the lowest contribution in winter ( $45.1 \pm 10.2\%$ ).  
196 The higher WSOC fraction in OC during summer is largely contributed by SOA and to some  
197 extent by biomass burning emissions because both SOA and biomass burning OA consist of

198 high fraction of WSOC (Ram et al., 2012; Yan et al., 2015; Daellenbach et al., 2016). The lower  
199 WSOC fractions in OC during winter could be attributed to enhanced emissions from coal  
200 combustion which produce a large fraction of water-insoluble organics (Daellenbach et al.,  
201 2016; Yan et al., 2017).  $Abs_{365,MSOC}$  is approximately 2 times (range 1.7-2.3) higher than  
202  $Abs_{365,WSOC}$ , which is similar to the results measured in Beijing (Cheng et al., 2016),  
203 southeastern Tibetan Plateau (Zhu et al., 2018), Gwangju, Korea (Park et al., 2018) and the  
204 Research Triangle Park, USA (Xie et al., 2019), indicating that the optical properties of BrC  
205 could be largely underestimated when using water as the extracting solvent as non-polar  
206 fraction of BrC is also important to light absorption of BrC (Sengupta et al., 2018). In Fig. S2  
207 we summarized those previously reported  $Abs_{365,WSOC}$  (as  $Abs_{365,MSOC}$  was not commonly  
208 measured in many previous studies) values at different sites in Asian urban and remote areas  
209 and the US.  $Abs_{365,WSOC}$  is significantly higher in most Asian urban regions than in the Asian  
210 remote sites and the US, and show clear seasonal variations. The high light absorption of BrC  
211 in Asian urban regions, especially during winter, may have important effects on regional climate  
212 and radiation forcing (Park et al., 2010; Laskin et al., 2015). As discussed in Feng et al. (2013),  
213 the average global climate forcing of BrC was estimated to be 0.04-0.11  $W m^{-2}$  and above 0.25  
214  $W m^{-2}$  in urban sites of south and east Asia regions, which is about 25% of the radiative forcing  
215 of black carbon (BC, 1.07  $W m^{-2}$ ). Thus, to further understand the influence of BrC on regional  
216 radiation forcing, it is essential to identify and quantify the sources of BrC in Asia.

217 The seasonal averages of AAE of water-soluble BrC were between 5.32 and 6.15 without  
218 clear seasonal trend (see Table S3). The seasonal averages of AAE of methanol-soluble BrC  
219 were relatively lower than those of water-soluble BrC, ranging from 4.45 to 5.18 which is  
220 similar to the results in Los Angeles Basin (Zhang et al., 2013) and Gwangju, Korea (Park et  
221 al., 2018). This is because methanol can extract more conjugated compounds that absorb  
222 strongly at longer wavelengths (e.g., PAHs) (Samburova et al., 2016). The AAE values of water-  
223 soluble BrC (as AAE of methanol-soluble BrC was not commonly measured in many previous  
224 studies) in urban, rural and remote regions show a large difference (see Fig. 2a), typically with  
225 much lower AAE values in urban regions than those in rural and remote regions, indicating the  
226 difference in sources and chemical composition of chromophores. The urban regions are mainly



227 affected by anthropogenic emissions. Therefore, urban BrC may contain a large amount of  
228 aromatic chromophores with high conjugation degree, which absorb light at a longer  
229 wavelength and have lower AAE values (Lambe et al., 2013; Wang et al., 2018).

230 The average MAE<sub>365</sub> values of water- and methanol-soluble BrC show large seasonal  
231 variations, with highest values in winter (1.85 and 1.50 m<sup>2</sup> gC<sup>-1</sup>, respectively), followed by fall  
232 (1.18 and 1.52 m<sup>2</sup> gC<sup>-1</sup>), spring (1.01 and 0.79 m<sup>2</sup> gC<sup>-1</sup>), and summer (0.91 and 1.21 m<sup>2</sup> gC<sup>-1</sup>).  
233 Such large seasonal differences indicate seasonal difference in BrC sources. For example,  
234 contributions from coal burning and biomass burning were much larger in winter than in other  
235 seasons due to large residential heating activities (also see Section 3.3 for more details).  
236 Compared to previous studies (Fig. 2b), the average values of MAE<sub>365,WSOC</sub> are obviously higher  
237 in urban sites than in rural and remote sites that are less influenced by anthropogenic activities.  
238 The higher MAE<sub>365,WSOC</sub> values in urban regions is likely associated with enhanced  
239 anthropogenic emissions from e.g., coal combustion and biomass burning, and the lower  
240 MAE<sub>365,WSOC</sub> values in rural and remote regions could be attributed to biogenic sources or aged  
241 secondary BrC (Lei et al., 2018; Xie et al., 2019).

### 242 **3.2 Chemical characterization of the BrC chromophores**

243 Given the complexity in emission sources and formation processes, the molecular  
244 composition of atmospheric BrC remains largely unknown. PAHs, NACs and MOPs have  
245 recently been found as major chromophores in biomass burning-derived BrC (Lin et al., 2016,  
246 2017, 2018). However, these compounds can also be directly emitted by coal combustion and  
247 motor vehicle or formed by secondary reactions (Harrison et al., 2005; Iinuma et al., 2010; Liu  
248 et al., 2017; Wang et al., 2018; Lu et al., 2019), making source attribution of atmospheric BrC  
249 more challenging. To obtain the exact molecular composition of BrC chromophores and  
250 understand the influence of a specific chromophore on BrC optical property, we measured the  
251 light absorption characteristics of available chromophore standards including 12 PAHs, 10  
252 NACs and 3 MOPs, and quantified their concentrations in PM<sub>2.5</sub> samples with GC-MS. The  
253 light absorption contribution of individual chromophores to that of methanol-soluble BrC in the  
254 wavelength range of 300-500 nm was estimated according to its concentration and mass  
255 absorption efficiency (see Supplementary). Fig. 3 shows the contribution of carbon content in

256 identified BrC chromophores to the total OC mass. They all show obvious seasonal variations  
257 with the highest values in winter and lowest in summer. The seasonal difference can be up to a  
258 factor of 5-6. The contribution of PAHs ranged from 0.12% in summer to 0.47% in winter,  
259 NACs from 0.02% in summer to 0.13% in winter, and MOPs from 0.01% in summer to 0.06%  
260 in winter. It should be noted that NACs are dominated by 4-nitrophenol and 4-nitrocatechol in  
261 spring, fall and winter, but by 4-nitrophenol and 5-nitrosalicylic acid in summer. The difference  
262 is likely due to enhanced summertime formation of 5-nitrosalicylic acid, which is more oxidized  
263 than other nitrated phenols measured in this study (Wang et al., 2018).

264 The seasonally averaged contributions of PAHs, NACs, MOPs and total measured  
265 chromophores to light absorption of methanol-soluble BrC between 300 to 500 nm are shown  
266 in Fig. 4. They show large seasonal variations and wavelength dependence. Specifically, PAHs  
267 made the largest contribution to BrC light absorption in fall, followed by winter, spring and  
268 summer, and show two large absorption peaks at about 365 nm and 380 nm, which are mainly  
269 associated with the absorption of BaP, BghiP, IcdP, FLU, BkF and BaA (see Fig. S3). Compared  
270 to PAHs, NACs show the largest contribution in winter, followed by fall, spring and summer,  
271 and exhibit only one absorption peak at about 320 nm in spring and summer and at about 330  
272 nm in fall and winter. The red shift in the absorption peak could be attributed to the increase of  
273 contributions from 4-nitrocatechol, 4-methyl-5-nitrocatechol and 3-methyl-5-nitrocatechol  
274 which have absorption peak at about 330-350 nm (see Fig. S3). Different from PAHs and NACs,  
275 MOPs contribute the most in winter, followed by spring, fall and summer, and only show one  
276 absorption peak at about 310 nm. The difference in light absorption contributions of different  
277 chromophores in different seasons reflects the difference in sources, emission strength and  
278 atmospheric formation processes.

279 The total contributions of PAHs, NACs and MOPs to the light absorption of methanol-  
280 soluble BrC ranged from 0.47% (summer) to 1.56% (winter) at the wavelength of 300-500 nm  
281 and ranged from 1.05% (summer) to 3.26% (winter) at the wavelength of 365 nm (see Table 1).  
282 The average contribution of PAHs to the BrC light absorption at 365 nm was 0.97% in summer  
283 (the lowest) and 2.69% in fall (the highest), the contribution of NACs was 0.09% in summer  
284 and 0.82% in winter, and the contribution of MOPs was 0.006% in summer and 0.024% in

285 winter. The low contributions of these measured chromophores to the light absorption of  
286 methanol-soluble BrC are consistent with previous studies. For example, Huang et al. (2018)  
287 measured 18 PAHs and their derivatives, which on average contributed ~1.7% of the overall  
288 absorption of methanol-soluble BrC in Xi'an. Mohr et al. (2013) estimated the contribution of  
289 five NACs to particulate BrC light absorption at 370 nm to be ~4% in Detling, UK. Zhang et  
290 al. (2013) measured eight NACs, which accounted for ~4% of water-soluble BrC absorption at  
291 365 nm in Los Angeles. Teich et al. (2017) determined eight NACs during six campaigns at five  
292 locations in summer and winter, and founded that the mean contribution of NACs to water-  
293 soluble BrC absorption at 370 nm ranged from 0.10% to 1.25% under acidic conditions and  
294 from 0.13% to 3.71% under alkaline conditions. Slightly different from these previous studies,  
295 we investigated the contributions of three groups of chromophores with different light-  
296 absorbing properties to the light absorption of BrC, and provided further understanding in the  
297 relationships between optical properties and chemical composition of BrC in the atmosphere.  
298 For example, vanillin, which has negligible contribution to BrC light absorption at 365 nm, can  
299 produce secondary BrC through oxidation and thus enhance the light absorption by a factor of  
300 5-7 (Li et al., 2014; Smith et al., 2016). The contribution of PAHs to the light absorption of  
301 methanol-soluble BrC at 365 nm was 5-13 times that of their mass fraction of carbon in OC, 6-  
302 9 times for NACs, and 0.4-0.7 times for MOPs (4-8 times at 310 nm for MOPs). These results  
303 further demonstrate that even a small amount of chromophores can have a disproportionately  
304 high impact on the light absorption properties of BrC, and that the light absorption of BrC is  
305 likely determined by a number of chromophores with strong light absorption ability (Kampf et  
306 al., 2012; Teich et al., 2017). Of note, a large fraction of BrC chromophores are still not  
307 identified so far, and more studies are therefore necessary to better understand the BrC  
308 chemistry. Based on laboratory and ambient studies, imidazoles (Kampf et al., 2012; Teich et  
309 al., 2016), quinones (Lee et al., 2014; Pillar et al., 2017), nitrogenous PAHs (Lin et al., 2016;  
310 Lin et al., 2018), polyphenols (Lin et al., 2016; Pillar et al., 2017) and oligomers with higher  
311 conjugation (Lin et al., 2014; Lavi et al., 2017) could be included in future studies.

### 312 **3.3 Sources of BrC**

313 Two approaches have been used to quantify the sources of BrC, including multiple linear

314 regression and receptor models such as PMF. For example, Washenfelder et al. (2015) utilized  
315 multiple linear regression to determine the contribution of individual OA factors resolved by  
316 PMF to OA light absorption in the southeastern America. Moschos et al. (2018) combined the  
317 time series of PMF-resolved OA factors with the time series of light absorption of water-soluble  
318 OA extract as model inputs to quantify the sources of BrC in Magadino and Zurich, Switzerland.  
319 Xie et al. (2019) quantified the sources of BrC in southeastern America using Abs<sub>365</sub>, elemental  
320 carbon (EC), OC, WSOC, isoprene sulfate ester, monoterpene sulfate ester, levoglucosan and  
321 isoprene SOA tracers as PMF model inputs. However, it should be noted that previous studies  
322 mainly rely on the correlation between measured light absorption and organic tracers that do  
323 not contain a BrC chromophore, and therefore may lead to bias in BrC source apportionment.  
324 To better constrain the sources of BrC (i.e., contribution to Abs<sub>365,MSOC</sub>), we used BrC  
325 chromophores as PMF model inputs. The inputs include vanillic acid, vanillin, and syringyl  
326 acetone for BrC from biomass burning, and FLU, PYR, CHR, BaA, BaP, BbF, BkF, IcdP, BghiP,  
327 for BrC from incomplete combustion and other light absorbing chromophores 9,10AQ, BEN,  
328 and BbF11O. In addition, we included commonly used markers levoglucosan for biomass  
329 burning, phthalic acid for secondary BrC, hopanes for vehicle emission and picene for coal  
330 burning in the model inputs.

331 Four factors were resolved, including vehicle emission, coal burning, biomass burning and  
332 secondary formation. The uncertainties for PMF analysis were < 10% for secondary formation  
333 and biomass burning, < 15% for vehicle emission and coal burning. The profile of each factor  
334 is shown in Fig. S4. The first factor is characterized by a high contribution of phthalic acid, a  
335 tracer of secondary formation of OA. The second factor is dominated by hopanes, mainly from  
336 vehicular emissions. The third factor is characterized by high contributions of PI, BaP, BbF,  
337 BkF, IcdP, BghiP, mainly from coal combustion emissions, while the fourth factor has high  
338 contributions of levoglucosan, vanillic acid, vanillin, syringyl acetone from biomass burning  
339 emissions. The seasonal difference in relative contribution of each factor to BrC light absorption  
340 is shown in Fig. 5. In spring, vehicular emissions (34%) and secondary formation (37%) were  
341 the main contributors to BrC and coal combustion also had a relatively large contribution (29%).  
342 In summer, secondary formation constituted the largest fraction (~60%), mainly due to

343 enhanced photochemical formation of secondary BrC. In fall, vehicular emissions (38%), coal  
344 combustion (29%) and biomass burning (22%) all had significant contributions to BrC. In  
345 winter, coal combustion (44%) and biomass burning (36%) were the main contributors, due to  
346 emissions from residential biomass burning (wood and crop residues) and coal combustion for  
347 heating. In terms of absolute contributions to absorption of MSOC at 365 nm (see Table S4),  
348 secondary formation contributed 1.75, 2.55, 1.70, 6.20 M m<sup>-1</sup> in spring, summer, fall and winter,  
349 respectively. The high contribution in winter can be attributed to abundant precursors (volatile  
350 organic compounds) co-emitted with other primary sources (especially coal burning and  
351 biomass burning), while the high contribution in summer might be due to strong photochemical  
352 activity. For spring and fall, the absolute contributions from secondary formation were very  
353 similar, indicating moderate precursor emission and moderate photochemical activity. Also it  
354 should be noted that the absolute contributions of vehicle emission to absorption of MSOC at  
355 365 nm were still higher in spring and fall than those in summer and winter, yet these differences  
356 by a factor of 2-9 are still less pronounced than the differences (spring/fall vs. winter) for other  
357 primary emissions (> 40 times for coal burning and > 25 times for biomass burning). In  
358 particular, the high vehicle contribution in fall might be affected by high relative humidity in  
359 fall (83% in fall vs. 61-69% in other seasons, on average) resulting in high vehicular PM<sub>2.5</sub>  
360 emissions (Chio et al., 2010). Such large seasonal difference in emission sources and  
361 atmospheric processes of BrC indicates that more studies are required to better understand the  
362 relationship between chemical composition, formation processes, and light absorption  
363 properties of BrC.

#### 364 **4 Conclusion**

365 The light absorption properties of water- and methanol-soluble BrC in different seasons  
366 were investigated in Xi'an. The light absorption coefficient of methanol-soluble BrC was  
367 approximately 2 times higher than that of water-soluble BrC at 365 nm, and had an average  
368 MAE<sub>365</sub> value of 1.27 ± 0.46 m<sup>2</sup> gC<sup>-1</sup>. The average MAE<sub>365</sub> value of water-soluble BrC was 1.19  
369 ± 0.51 m<sup>2</sup> gC<sup>-1</sup>, which is comparable to those in previous studies at urban sites but higher than  
370 those in rural and remote areas. The seasonally averaged AAE values of water-soluble BrC  
371 ranged from 5.32 to 6.15, which are higher than those of methanol-soluble BrC (between 4.45

372 and 5.18). In combination with previous studies, we found that AAE values of water-soluble  
373 BrC were much lower in urban regions than those in rural and remote regions. The difference  
374 of optical properties of BrC in different regions could be attributed to the difference in sources  
375 and chemical composition of BrC chromophores. The contributions of 12 PAHs, 10 NACs and  
376 3 MOPs to the light absorption of methanol-soluble BrC were determined and showed large  
377 seasonal variations. Specifically, the total contribution to methanol-soluble BrC light absorption  
378 at 365 nm ranged from 1.1% to 3.3%, which is 5-7 times higher than their carbon mass fractions  
379 in total OC. This result indicates that the light absorption of BrC is likely determined by an  
380 amount of chromophores with strong light absorption ability. Four major sources of methanol-  
381 soluble BrC were identified, including secondary formation, vehicle emission, coal combustion  
382 and biomass burning. On average, secondary formation and vehicular emission were the main  
383 contributors of BrC in spring (~70%). Vehicular emission (38%), coal burning (29%) and  
384 biomass burning (22%) all contributed significantly to BrC in fall. Coal combustion and  
385 biomass burning were the major contributors in winter (~80%), and secondary formation was  
386 the predominant source in summer (~60%). The large variations of BrC sources in different  
387 seasons suggest that more studies are needed to understand the seasonal difference in chemical  
388 composition, formation processes, and light absorption properties of BrC, as well as their  
389 relationships.

## 390 **5 Abbreviations of organics**

### 391 **PAHs (Polycyclic Aromatic Hydrocarbons)**

392	BaA	Benzo(a)anthracene
393	BaP	Benzo(a)pyrene
394	BbF	Benzo(b)fluoranthene
395	BbF11O	Benzo[b]fluoren-11-One
396	BEN	Benzanthrone
397	BghiP	Benzo(ghi)perylene
398	BkF	Benzo(k)fluoranthene
399	CHR	Chrysene

400	FLU	Fluoranthene
401	IcdP	Indeno[1,2,3-cd]pyrene
402	PYR	Pyrene
403	9,10AQ	9,10-Anthracenequinone
404	<b>NACs (Nitrated Aromatic Compounds)</b>	
405	2M4NP	2-Methyl-4-Nitrophenol
406	2,6DM4NP	2,6-Dimethyl-4-Nitrophenol
407	3M4NP	3-Methyl-4-Nitrophenol
408	3M5NC	3-Methyl-5-Nitrocatechol
409	3NSA	3-Nitrosalicylic Acid
410	4M5NC	4-Methyl-5-Nitrocatechol
411	4NC	4-Nitrocatechol
412	4NP	4-Nitrophenol
413	4N1N	4-Nitro-1-Naphthol
414	5NSA	5-Nitrosalicylic Acid
415	<b>MOP (Methoxyphenols)</b>	
416	SyA	Syringyl Acetone
417	VaA	Vanillic Acid
418	VAN	Vanillin
419	<b>Hopanes</b>	
420	HP1	17 $\alpha$ (H),21 $\beta$ (H)-30-Norhopane
421	HP2	17 $\alpha$ (H),21 $\beta$ (H)-Hopane
422	HP3	17 $\alpha$ (H),21 $\beta$ (H)-(22S)-Homohopane
423	HP4	17 $\alpha$ (H),21 $\beta$ (H)-(22R)-Homohopane

424 *Data availability.* Raw data used in this study are archived at the Institute of Earth Environment,  
425 Chinese Academy of Sciences, and are available on request by contacting the corresponding

426 author.

427 *Supplement.* The Supplement related to this article is available online at

428 *Author contributions.* RJH designed the study. Data analysis was done by WY, LY, and RJH.  
429 WY, LY and RJH interpreted data, prepared the display items and wrote the manuscript. All  
430 authors commented on and discussed the manuscript.

431 *Acknowledgements.* This work was supported by the National Natural Science Foundation of  
432 China (NSFC) under grant no. 41877408, 41925015, and no. 91644219, the Chinese Academy  
433 of Sciences (no. ZDBS-LY-DQC001), the Cross Innovative Team fund from the State Key  
434 Laboratory of Loess and Quaternary Geology (SKLLQG) (no. SKLLQGTD1801), and the  
435 National Key Research and Development Program of China (no. 2017YFC0212701). Yongjie  
436 Li acknowledges funding support from the National Natural Science Foundation of China  
437 (41675120), the Science and Technology Development Fund, Macau SAR (File no.  
438 016/2017/A1), and the Multi-Year Research grant (No. MYRG2018-00006-FST) from the  
439 University of Macau.

#### 440 **References**

441 Al-Naiema, I. M., and Stone, E. A.: Evaluation of anthropogenic secondary organic aerosol  
442 tracers from aromatic hydrocarbons, *Atmos. Chem. Phys.*, 17, 2053-2065,  
443 doi:10.5194/acp-17-2053-2017, 2017.

444 Bandowe, B. A. M., Meusel, H., Huang, R.-J., Ho, K., Cao, J., Hoffmann, T., and Wilcke, W.:  
445 PM<sub>2.5</sub>-bound oxygenated PAHs, nitro-PAHs and parent-PAHs from the atmosphere of a  
446 Chinese megacity: Seasonal variation, sources and cancer risk assessment, *Sci. Total*  
447 *Environ.*, 473-474, 77-87, 2014.

448 Bosch, C., Andersson, A., Kirillova, E. N., Budhavant, K., Tiwari, S., Praveen, P. S., Russell,  
449 L. M., Beres, N. D., Ramanathan, V., and Gustafsson, Ö.: Source-diagnostic dual-isotope  
450 composition and optical properties of water-soluble organic carbon and elemental carbon  
451 in the South Asian outflow intercepted over the Indian Ocean, *J. Geophys. Res. Atmos.*,  
452 119, 11743-11759, doi:10.1002/2014JD022127, 2014.



453 Chen, Y., and Bond, T. C.: Light absorption by organic carbon from wood combustion, *Atmos.*  
454 *Chem. Phys.*, 10, 1773-1787, doi:10.5194/acp-10-1773-2010, 2010.

455 Chen, Y., Ge, X., Chen, H., Xie, X., Chen, Y., Wang, J., Ye, Z., Bao, M., Zhang, Y., and Chen,  
456 M.: Seasonal light absorption properties of water-soluble brown carbon in atmospheric  
457 fine particles in Nanjing, China, *Atmos. Environ.*, 187, 230-240,  
458 doi:10.1016/j.atmosenv.2018.06.002, 2018.

459 Cheng, Y., He, K. B., Du, Z. Y., Engling, G., Liu, J. M., Ma, Y. L., Zheng, M., and Weber, R. J.:  
460 The characteristics of brown carbon aerosol during winter in Beijing, *Atmos. Environ.*,  
461 127, 355-364, doi:10.1016/j.atmosenv.2015.12.035, 2016.

462 Choi, D., Beardsley, M., Brzezinski, D., Koupal, J., and Warila, J.: MOVES sensitivity analysis:  
463 the impacts of temperature and humidity on emissions, [online] Available from:  
464 <https://www3.epa.gov/ttnchie1/conference/ei19/session6/choi.pdf>, 2010.

465 Chow, J. C., Watson, J. G., Robles, J., Wang, X. L., Antony Chen, L. W., Trimble, D. L., Kohl,  
466 S. D., Tropp, R. J., and Fung, K. K.: Quality assurance and quality control for  
467 thermal/optical analysis of aerosol samples for organic and elemental carbon, *Anal.*  
468 *Bioanal. Chem.*, 401, 3141- 3152, doi:10.1007/s00216-011-5103-3, 2011.

469 Chow, K. S., Huang, X. H. H., and Yu, J. Z.: Quantification of nitroaromatic compounds in  
470 atmospheric fine particulate matter in Hong Kong over 3 years: field measurement  
471 evidence for secondary formation derived from biomass burning emissions, *Environ.*  
472 *Chem.*, 13, 665-673, doi:10.1071/EN15174, 2015.

473 Canonaco, F., Crippa, M., Slowik, J. G., Baltensperger, U., and Prévôt, A. S. H.: SoFi, an IGOR  
474 based interface for the efficient use of the generalized multilinear engine (ME-2) for the  
475 source apportionment: ME-2 application to aerosol mass spectrometer data, *Atmos. Meas.*  
476 *Tech.*, 6, 3649-3661, doi:10.5194/amt-6-3649-2013, 2013.

477 Daellenbach, K. R., Bozzetti, C., Krepeleva, A. K., Canonaco, F., Wolf, R., Zotter, P., Fermo,  
478 P., Crippa, M., Slowik, J. G., Sosedova, Y., Zhang, Y., Huang, R. J., Poulain, L., Szidat, S.,  
479 Baltensperger, U., El Haddad, I., and Prevot, A. S. H.: Characterization and source  
480 apportionment of organic aerosol using offline aerosol mass spectrometry, *Atmos. Meas.*  
481 *Tech.*, 9, 23-39, doi:10.5194/amt-9-23-2016, 2016.

482 De Haan, D. O., Corrigan, A. L., Smith, K. W., Stroik, D. R., Turley, J. J., Lee, F. E., Tolbert,  
483 M. A., Jimenez, J. L., Cordova, K. E., and Ferrell, G. R.: Secondary organic aerosol-  
484 forming reactions of glyoxal with amino acids, *Environ. Sci. Technol.*, 43, 2818-2824,  
485 doi:10.1021/es803534f, 2009.

486 De Haan, D. O., Hawkins, L. N., Kononenko, J. A., Turley, J. J., Corrigan, A. L., Tolbert, M.  
487 A., and Jimenez, J. L.: Formation of nitrogen-containing oligomers by methylglyoxal and  
488 amines in simulated evaporating cloud droplets, *Environ. Sci. Technol.*, 45, 984-991,  
489 doi:10.1021/es102933x, 2011.

490 Feng, Y., Ramanathan, V., and Kotamarthi, V. R.: Brown carbon: A significant atmospheric  
491 absorber of solar radiation?, *Atmos. Chem. Phys.*, 13, 8607-8621, doi:10.5194/acp-13-  
492 8607-2013, 2013.

493 Flores, J. M., Washenfelder, R. A., Adler, G., Lee, H. J., Segev, L., Laskin, J., Laskin, A.,  
494 Nizkorodov, S. A., Brown, S. S., and Rudich, Y.: Complex refractive indices in the near-  
495 ultraviolet spectral region of biogenic secondary organic aerosol aged with ammonia, *Phys.*  
496 *Chem. Chem. Phys.*, 16, 10629-10642, doi:10.1039/c4cp01009d, 2014.

497 Gilardoni, S., Massoli, P., Paglione, M., Giulianelli, L., Carbone, C., Rinaldi, M., Decesari, S.,  
498 Sandrini, S., Costabile, F., Gobbi, G. P., Pietrogrande, M. C., Visentin, M., Scotto, F., Fuzzi,  
499 S., and Facchini, M. C.: Direct observation of aqueous secondary organic aerosol from  
500 biomass-burning emissions, *Proc. Natl. Acad. Sci.*, 113, 10013-10018,  
501 doi:10.1073/pnas.1602212113, 2016.

502 Harrison, M. A. J., Barra, S., Borghesi, D., Vione, D., Arsene, C., and Olariu, R. I.: Nitrated  
503 phenols in the atmosphere: a review, *Atmos. Environ.*, 39, 231-248,  
504 doi:10.1016/j.atmosenv.2004.09.044, 2005.

505 Hecobian, A., Zhang, X., Zheng, M., Frank, N. H., Edgerton, E. S., and Weber, R. J.: Water-  
506 soluble organic aerosol material and the light absorption characteristics of aqueous extracts  
507 measured over the Southeastern United States, *Atmos. Chem. Phys.*, 10, 5965-5977,  
508 doi:10.5194/acp-10-5965-2010, 2010.

509 Ho, K. F., Ho, S. S. H., Huang, R. J., Liu, S. X., Cao, J. J., Zhang, T., Chuang, H. C., Chan, C.  
510 S., Hu, D., and Tian, L.: Characteristics of water-soluble organic nitrogen in fine

511 particulate matter in the continental area of China, *Atmos. Environ.*, 106, 252-261,  
512 doi:10.1016/j.atmosenv.2015.02.010, 2015.

513 Huang, R. J., Zhang, Y. L., Bozzetti, C., Ho, K. F., Cao, J. J., Han, Y. M., Daellenbach, K. R.,  
514 Slowik, J. G., Platt, S. M., Canonaco, F., Zotter, P., Wolf, R., Pieber, S. M., Bruns, E. A.,  
515 Crippa, M., Ciarelli, G., Piazzalunga, A., Schwikowski, M., Abbaszade, G., Schnelle-Kreis,  
516 J., Zimmermann, R., An, Z. S., Szidat, S., Baltensperger, U., El Haddad, I., and Prévôt, A.  
517 S. H.: High secondary aerosol contribution to particulate pollution during haze events in  
518 China, *Nature*, 514, 218-222, 2014.

519 Huang, R. J., Yang, L., Cao, J., Chen, Y., Chen, Q., Li, Y., Duan, J., Zhu, C., Dai, W., Wang, K.,  
520 Lin, C., Ni, H., Corbin, J. C., Wu, Y., Zhang, R., Tie, X., Hoffmann, T., O'Dowd, C., and  
521 Dusek, U.: Brown carbon aerosol in urban Xi'an, Northwest China: the composition and  
522 light absorption properties, *Environ. Sci. Technol.*, 52, 6825-6833,  
523 doi:10.1021/acs.est.8b02386, 2018.

524 Iinuma, Y., Böge, O., Gräfe, R., and Herrmann, H.: Methyl-nitrocatechols: atmospheric tracer  
525 compounds for biomass burning secondary organic aerosols, *Environ. Sci. Technol.*, 44,  
526 8453-8459, doi:10.1021/Es102938a, 2010.

527 Jacobson, M. Z.: Isolating nitrated and aromatic aerosols and nitrated aromatic gases as sources  
528 of ultraviolet light absorption, *J. Geophys. Res.*, 104, 3527-3542,  
529 doi:10.1029/1998jd100054, 1999.

530 Kampf, C. J., Jakob, R., and Hoffmann, T.: Identification and characterization of aging products  
531 in the glyoxal/ammonium sulfate system - implications for light-absorbing material in  
532 atmospheric aerosols, *Atmos. Chem. Phys.*, 12, 6323-6333, doi:10.5194/acp-12-6323-  
533 2012, 2012.

534 Kirillova, E. N., Andersson, A., Han, J., Lee, M., and Gustafsson, Ö.: Sources and light  
535 absorption of water-soluble organic carbon aerosols in the outflow from northern China,  
536 *Atmos. Chem. Phys.*, 14, 1413-1422, 2014a.

537 Kirillova, E. N., Andersson, A., Tiwari, S., Srivastava, A. K., Bisht, S. D., and Gustafsson, Ö.:  
538 Water-soluble organic carbon aerosols during a full New Delhi winter: Isotope-based  
539 source apportionment and optical properties, *J. Geophys. Res. Atmos.*, 119, 3476-3485,

540 2014b.

541 Lambe, A. T., Cappa, C. D., Massoli, P., Onasch, T. B., Forestieri, S. D., Martin, A. T.,  
542 Cummings, M. J., Croasdale, D. R., Brune, W. H., Worsnop, D. R., and Davidovits, P.:  
543 Relationship between oxidation level and optical properties of secondary organic aerosol,  
544 *Environ. Sci. Technol.*, 47, 6349-6357, doi:10.1021/es401043j, 2013.

545 Laskin, A., Laskin, J., and Nizkorodov, S. A.: Chemistry of atmospheric brown carbon, *Chem.*  
546 *Rev.*, 115, 4335-4382, doi:10.1021/cr5006167, 2015.

547 Lavi, A., Lin, P., Bhaduri, B., Carmieli, R., Laskin, A., and Rudich, Y.: Characterization of  
548 Light-Absorbing Oligomers from Reactions of Phenolic Compounds and Fe(III), *ACS*  
549 *Earth and Space Chemistry*, 1, 637-646, 2017.

550 Lee, H. J., Aiona, P. K., Laskin, A., Laskin, J., and Nizkorodov, S. A.: Effect of solar radiation  
551 on the optical properties and molecular composition of laboratory proxies of atmospheric  
552 brown carbon, *Environ. Sci. Technol.*, 48, 10217-10226, 2014.

553 Lei, Y. L., Shen, Z. X., Wang, Q. Y., Zhang, T., Cao, J. J., Sun, J., Zhang, Q., Wang, L. Q., Xu,  
554 H. M., Tian, J., and Wu, J. M.: Optical characteristics and source apportionment of brown  
555 carbon in winter PM<sub>2.5</sub> over Yulin in Northern China, *Atmos. Res.*, 213, 27-33,  
556 doi:10.1016/j.atmosres.2018.05.018, 2018.

557 Li, G., Bei, N., Tie, X., and Molina, L. T.: Aerosol effects on the photochemistry in Mexico  
558 City during MCMA-2006/MILAGRO campaign, *Atmos. Chem. Phys.*, 11, 5169-5182,  
559 doi:10.5194/acp-11-5169-2011, 2011.

560 Li, M. J., Fan, X. J., Zhu, M. B., Zou, C. L., Song, J. Z., Wei, S. Y., Jia, W. L., and Peng, P. A.:  
561 Abundance and Light Absorption Properties of Brown Carbon Emitted from Residential  
562 Coal Combustion in China, *Environ. Sci. Technol.*, 53, 595-603, 2019.

563 Li, Y. J., Huang, D. D., Cheung, H. Y., Lee, A. K. Y., and Chan, C. K.: Aqueous-phase  
564 photochemical oxidation and direct photolysis of vanillin - a model compound of methoxy  
565 phenols from biomass burning, *Atmos. Chem. Phys.*, 14, 2871-2885, doi:10.5194/acp-14-  
566 2871-2014, 2014.

567 Lin, Y., Budisulistiorini, S. H., Chu, K., Siejack, R. A., Zhang, H., Riva, M., Zhang, Z., Gold,  
568 A., Kautzman, K. E., and Surratt, J. D.: Light-Absorbing Oligomer Formation in

569 Secondary Organic Aerosol from Reactive Uptake of Isoprene Epoxydiols, *Environ. Sci.*  
570 *Technol.*, 48, 12012-12021, doi:10.1021/es503142b, 2014.

571 Lin, P., Aiona, P. K., Li, Y., Shiraiwa, M., Laskin, J., Nizkorodov, S. A., and Laskin, A.:  
572 Molecular characterization of brown carbon in biomass burning aerosol particles, *Environ.*  
573 *Sci. Technol.*, 50, 11815-11824, doi:10.1021/acs.est.6b03024, 2016.

574 Lin, P., Bluvshstein, N., Rudich, Y., Nizkorodov, S. A., Laskin, J., and Laskin, A.: Molecular  
575 chemistry of atmospheric brown carbon inferred from a nationwide biomass burning event,  
576 *Environ. Sci. Technol.*, 51, 11561-11570, doi:10.1021/acs.est.7b02276, 2017.

577 Lin, P., Fleming, L. T., Nizkorodov, S. A., Laskin, J., and Laskin, A.: Comprehensive Molecular  
578 Characterization of Atmospheric Brown Carbon by High Resolution Mass Spectrometry  
579 with Electrospray and Atmospheric Pressure Photoionization, *Anal. Chem.*, 90, 12493-  
580 12502, doi:10.1021/acs.analchem.8b02177, 2018.

581 Liu, Y., Yan, C. Q., Ding, X., Wang, X. M., Fu, Q. Y., Zhao, Q. B., Zhang, Y. H., Duan, Y. S.,  
582 Qiu, X. H., and Zheng, M.: Sources and spatial distribution of particulate polycyclic  
583 aromatic hydrocarbons in Shanghai, China, *Sci. Total Environ.*, 584-585, 307-317,  
584 doi:10.1016/j.scitotenv.2016.12.134, 2017.

585 Lu, C., Wang, X., Li, R., Gu, R., Zhang, Y., Li, W., Gao, R., Chen, B., Xue, L., and Wang, W.:  
586 Emissions of fine particulate nitrated phenols from residential coal combustion in China,  
587 *Atmos. Environ.*, 203, 10-17, doi:10.1016/j.atmosenv.2019.01.047, 2019.

588 Lu, J. W., Michel Flores, J., Lavi, A., Abo-Riziq, A., and Rudich, Y.: Changes in the optical  
589 properties of benzo[a]pyrene-coated aerosols upon heterogeneous reactions with NO<sub>2</sub> and  
590 NO<sub>3</sub>, *Phys. Chem. Chem. Phys.*, 13, 6484-6492, doi:10.1039/C0CP02114H, 2011.

591 Mohr, C., Lopez-Hilfiker, F. D., Zotter, P., Prevot, A. S. H., Xu, L., Ng, N. L., Herndon, S. C.,  
592 Williams, L. R., Franklin, J. P., Zahniser, M. S., Worsnop, D. R., Knighton, W. B., Aiken,  
593 A. C., Gorkowski, K. J., Dubey, M. K., Allan, J. D., and Thornton, J. A.: Contribution of  
594 nitrated phenols to wood burning brown carbon light absorption in Detling, United  
595 Kingdom during winter time, *Environ. Sci. Technol.*, 47, 6316-6324,  
596 doi:10.1021/es400683v, 2013.

597 Moise, T., Flores, J. M., and Rudich, Y.: Optical properties of secondary organic aerosols and

598 their changes by chemical processes, *Chem. Rev.*, 115, 4400-4439, doi:10.1021/cr5005259,  
599 2015.

600 Mok, J., Krotkov, N. A., Arola, A., Torres, O., Jethva, H., Andrade, M., Labow, G., Eck, T. F.,  
601 Li, Z., Dickerson, R. R., Stenchikov, G. L., Osipov, S., and Ren, X.: Impacts of brown  
602 carbon from biomass burning on surface UV and ozone photochemistry in the Amazon  
603 Basin, *Sci. Rep.*, 6, 36940, doi:10.1038/srep36940, 2016.

604 Moschos, V., Kumar, N. K., Daellenbach, K. R., Baltensperger, U., Prévôt, A. S. H., and El  
605 Haddad, I.: Source Apportionment of Brown Carbon Absorption by Coupling Ultraviolet-  
606 Visible Spectroscopy with Aerosol Mass Spectrometry, *Environ. Sci. Tech. Lett.*, 5, 302-  
607 308, doi:10.1021/acs.estlett.8b00118, 2018.

608 Nguyen, T. B., Laskin, A., Laskin, J., and Nizkorodov, S. A.: Brown carbon formation from  
609 ketoaldehydes of biogenic monoterpenes, *Faraday Discuss.*, 165, 473-494,  
610 doi:10.1039/C3FD00036B, 2013.

611 Ni, H. Y., Huang, R. J., Cao, J. J., Liu, W. G., Zhang, T., Wang, M., Meijer, H. A. J., and Dusek,  
612 U.: Source apportionment of carbonaceous aerosols in Xi'an, China: insights from a full  
613 year of measurements of radiocarbon and the stable isotope  $^{13}\text{C}$ , *Atmos. Chem. Phys.*, 18,  
614 16363-16383, doi:10.5194/acp-18-16363-2018, 2018.

615 Paatero, P.: Least squares formulation of robust non-negative factor analysis, *Chemom. Intell.*  
616 *Lab.*, 37, 23-35, doi:10.1016/S0169-7439(96)00044-5, 1997.

617 Park, R. J., Kim, M. J., Jeong, J. I., Yooun, D., and Kim, S.: A contribution of brown carbon  
618 aerosol to the aerosol light absorption and its radiative forcing in East Asia, *Atmos.*  
619 *Environ.*, 44, 1414-1421, doi:10.1016/j.atmosenv.2010.01.042, 2010.

620 Park, S., Yu, G. H., and Lee, S.: Optical absorption characteristics of brown carbon aerosols  
621 during the KORUS-AQ campaign at an urban site, *Atmos. Res.*, 203, 16-27,  
622 doi:10.1016/j.atmosres.2017.12.002, 2018.

623 Pillar, E. A., and Guzman, M. I.: Oxidation of substituted catechols at the air-water interface:  
624 Production of carboxylic acids, quinones, and polyphenols, *Environ. Sci. Technol.*, 51,  
625 4951- 4959, <https://doi.org/10.1021/acs.est.7b00232>, 2017.

626 Ram, K., Sarin, M. M., and Tripathi, S. N.: Temporal trends in atmospheric  $\text{PM}_{2.5}$ ,  $\text{PM}_{10}$ ,

627 elemental carbon, organic carbon, water-soluble organic carbon, and optical properties:  
628 impact of biomass burning emissions in the Indo-Gangetic Plain, *Environ. Sci. Technol.*,  
629 46, 686-695, doi:10.1021/es202857w, 2012.

630 Samburova, V., Connolly, J., Gyawali, M., Yatavelli, R. L. N., Watts, A. C., Chakrabarty, R. K.,  
631 Zielinska, B., Moosmüller, H., and Khlystov, A.: Polycyclic aromatic hydrocarbons in  
632 biomass-burning emissions and their contribution to light absorption and aerosol toxicity,  
633 *Sci. Total Environ.*, 568, 391-401, doi:10.1016/j.scitotenv.2016.06.026, 2016.

634 Samburova, V., Connolly, J., Gyawali, M., Yatavelli, R. L. N., Watts, A. C., Chakrabarty, R. K.,  
635 Zielinska, B., Moosmüller, H., and Khlystov, A.: Polycyclic aromatic hydrocarbons in  
636 biomass-burning emissions and their contribution to light absorption and aerosol toxicity,  
637 *Sci. Total Environ.*, 568, 391-401, doi:10.1016/j.scitotenv.2016.06.026, 2016.

638 Sengupta, D., Samburova, V., Bhattarai, C., Kirillova, E., Mazzoleni, L., Iaukea-Lum, M.,  
639 Watts, A., Moosmüller, H., and Khlystov, A.: Light absorption by polar and non-polar  
640 aerosol compounds from laboratory biomass combustion, *Atmos. Chem. Phys.*, 18, 10849-  
641 10867, doi:10.5194/acp-18-10849-2018, 2018.

642 Shapiro, E. L., Szprengiel, J., Sareen, N., Jen, C. N., Giordano, M. R., and McNeill, V. F.: Light-  
643 absorbing secondary organic material formed by glyoxal in aqueous aerosol mimics,  
644 *Atmos. Chem. Phys.*, 9, 2289-2300, doi:10.5194/acp-9-2289-2009, 2009.

645 Shen, M. L., Xing, J., Ji, Q. P., Li, Z. H., Wang, Y. H., Zhao, H. W., Wang, Q. R., Wang, T., Yu,  
646 L. W., Zhang, X. C., Sun, Y. X., Zhang, Z. H., Niu, Y., Wang, H. Q., Chen, W., Dai, Y. F.,  
647 Su, W. G., and Duan, H. W.: Declining Pulmonary Function in Populations with Long-  
648 term Exposure to Polycyclic Aromatic Hydrocarbons-Enriched PM<sub>2.5</sub>, *Environ. Sci.*  
649 *Technol.*, 52, 6610-6616, 2018.

650 Smith, J. D., Kinney, H., and Anastasio, C.: Phenolic carbonyls undergo rapid aqueous  
651 photodegradation to form low-volatility, light-absorbing products, *Atmos. Environ.*, 126,  
652 36-44, doi:10.1016/j.atmosenv.2015.11.035, 2016.

653 Song, J. Z., Li, M. J., Fan, X. J., Zou, C. L., Zhu, M. B., Jiang, B., Yu, Z. Q., Jia, W. L., Liao,  
654 Y. H., and Peng, P. A.: Molecular Characterization of Water- and Methanol-Soluble  
655 Organic Compounds Emitted from Residential Coal Combustion Using Ultrahigh-

656 Resolution Electrospray Ionization Fourier Transform Ion Cyclotron Resonance Mass  
657 Spectrometry, *Environ. Sci. Technol.*, 53, 13607-13617, doi:10.1021/acs.est.9b04331,  
658 2019.

659 Srinivas, B., and Sarin, M. M.: Light-absorbing organic aerosols (brown carbon) over the  
660 tropical Indian Ocean: impact of biomass burning emissions, *Environ. Res. Lett.*, 8,  
661 044042, doi:10.1088/1748-9326/8/4/044042, 2013.

662 Sun, J., Zhi, G., Hitzenberger, R., Chen, Y., Tian, C., Zhang, Y., Feng, Y., Cheng, M., Zhang, Y.,  
663 Cai, J., Chen, F., Qiu, Y., Jiang, Z., Li, J., Zhang, G., and Mo, Y.: Emission factors and  
664 light absorption properties of brown carbon from household coal combustion in China,  
665 *Atmos. Chem. Phys.*, 17, 4769-4780, doi:10.5194/acp-17-4769-2017, 2017.

666 Teich, M., van Pinxteren, D., Kecorius, S., Wang, Z., and Herrmann, H.: First quantification of  
667 imidazoles in ambient aerosol particles: potential photosensitizers, brown carbon  
668 constituents, and hazardous components, *Environ. Sci. Technol.*, 50, 1166-1173, 2016.

669 Teich, M., van Pinxteren, D., Wang, M., Kecorius, S., Wang, Z., Müller, T., Mocnik, G., and  
670 Herrmann, H.: Contributions of nitrated aromatic compounds to the light absorption of  
671 water-soluble and particulate brown carbon in different atmospheric environments in  
672 Germany and China, *Atmos. Chem. Phys.*, 17, 1653-1672, doi:10.5194/acp-17-1653-2017,  
673 2017.

674 Wang, G. H., Kawamura, K., Lee, S., Ho, K. F., and Cao, J. J.: Molecular, seasonal, and spatial  
675 distributions of organic aerosols from fourteen Chinese cities, *Environ. Sci. Technol.*, 40,  
676 4619-4625, doi:10.1021/es060291x, 2006.

677 Wang, J. Z., Ho, S. S. H., Huang, R. J., Gao, M. L., Liu, S. X., Zhao, S. Y., Cao, J. J., Wang, G.  
678 H., Shen, Z. X., and Han, Y. M.: Characterization of parent and oxygenated-polycyclic  
679 aromatic hydrocarbons (PAHs) in Xi'an, China during heating period: An investigation of  
680 spatial distribution and transformation, *Chemosphere*, 159, 367-377,  
681 doi:10.1016/j.chemosphere.2016.06.033, 2016.

682 Wang, L. W., Wang, X. F., Gu, R. R., Wang, H., Yao, L., Wen, L., Zhu, F. P., Wang, W. H., Xue,  
683 L. K., Yang, L. X., Lu, K. D., Chen, J. M., Wang, T., Zhang, Y. H., and Wang, W. X.:  
684 Observations of fine particulate nitrated phenols in four sites in northern China:



685 concentrations, source apportionment, and secondary formation, *Atmos. Chem. Phys.*, 18,  
686 4349-4359, doi:10.5194/acp-18-4349-2018, 2018.

687 Washenfelder, R. A., Attwood, A. R., Brock, C. A., Guo, H., Xu, L., Weber, R. J., Ng, N. L.,  
688 Allen, H. M., Ayres, B. R., Baumann, K., Cohen, R. C., Draper, D. C., Duffey, K. C.,  
689 Edgerton, E., Fry, J. L., Hu, W. W., Jimenez, J. L., Palm, B. B., Romer, P., Stone, E. A.,  
690 Wooldridge, P. J., and Brown, S. S.: Biomass burning dominates brown carbon absorption  
691 in the rural southeastern United States, *Geophys. Res. Lett.*, doi:10.1002/2014GL062444,  
692 42, 653-664, 2015.

693 Xie, M. J., Chen, X., Hays, M. D., Lewandowski, M., Offenberg, J., Kleindienst, T. E., and  
694 Holder, A. L.: Light absorption of secondary organic aerosol: composition and  
695 contribution of nitroaromatic compounds, *Environ. Sci. Technol.*, 51, 11607-11616,  
696 doi:10.1021/acs.est.7b03263, 2017.

697 Xie, M. J., Chen, X., Holder, A. L., Hays, M. D., Lewandowski, M., Offenberg, J. H.,  
698 Kleindienst, T. E., Jaoui, M., and Hannigan, M. P.: Light absorption of organic carbon and  
699 its sources at a southeastern U.S. location in summer, *Environ. Pollut.*, 244, 38-46,  
700 doi:10.1016/j.envpol.2018.09.125, 2019.

701 Yan, C. Q., Zheng, M., Sullivan, A. P., Bosch, C., Desyaterik, Y., Andersson, A., Li, X. Y., Guo,  
702 X. S., Zhou, T., Gustafsson, O., and Collett Jr, J. L.: Chemical characteristics and light-  
703 absorbing property of water-soluble organic carbon in Beijing: Biomass burning  
704 contributions, *Atmos. Environ.*, 121, 4-12, doi:10.1016/j.atmosenv.2015.05.005, 2015.

705 Yan, C. Q., Zheng, M., Bosch, C., Andersson, A., Desyaterik, Y., Sullivan, A. P., Collett, J. L.,  
706 Zhao, B., Wang, S. X., He, K. B., and Gustafsson, Ö.: Important fossil source contribution  
707 to brown carbon in Beijing during winter, *Sci. Rep.*, 7, 43182, doi:10.1038/srep43182,  
708 2017.

709 Zhang, X., Lin, Y.-H., Surratt, J. D., and Weber, R.: Sources, composition and absorption  
710 Ångström exponent of light-absorbing organic components in aerosol extracts from the  
711 Los Angeles Basin, *Environ. Sci. Technol.*, 47, 3685-3693, doi:10.1021/es305047b, 2013.

712 Zhang, Y., Forrister, H., Liu, J., Dibb, J., Anderson, B., Schwarz, J. P., Perring, A. E., Jimenez,  
713 J. L., Campuzano-Jost, P., Wang, Y., Nenes, A., and Weber, R. J.: Top-of-atmosphere

714 radiative forcing affected by brown carbon in the upper troposphere, *Nat. Geosci.*, 10, 486-  
715 489, doi:10.1038/NGEO2960, 2017a.

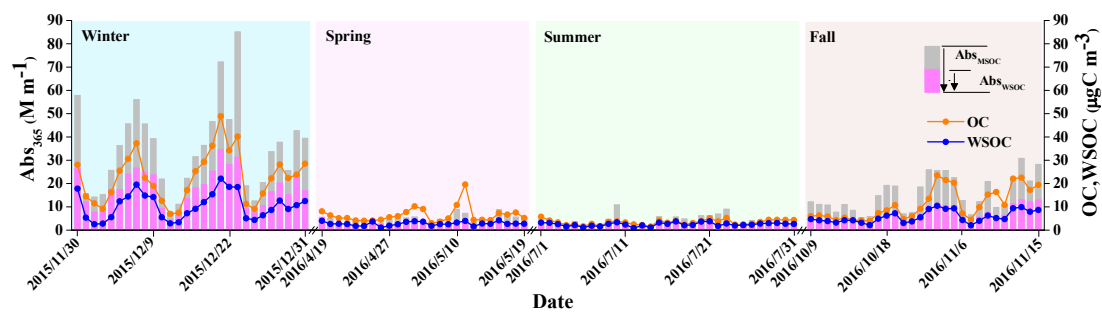
716 Zhang, Y., Xu, J., Shi, J., Xie, C., Ge, X., Wang, J., Kang, S., and Zhang, Q.: Light absorption  
717 by water-soluble organic carbon in atmospheric fine particles in the central Tibetan Plateau,  
718 *Environ. Sci. Pollut. Res.*, 24, 21386–21397, doi:10.1007/s11356-017-9688-8, 2017b.

719 Zhong, M., and Jang, M.: Dynamic light absorption of biomass-burning organic carbon  
720 photochemically aged under natural sunlight, *Atmos. Chem. Phys.*, 14, 1517-1525, 2014.

721 Zhu, C. S., Cao, J. J., Huang, R. J., Shen, Z. X., Wang, Q. Y., and Zhang, N. N.: Light absorption  
722 properties of brown carbon over the southeastern Tibetan Plateau, *Sci. Total Environ.*, 625,  
723 246-251, doi:10.1016/j.scitotenv.2017.12.183, 2018.

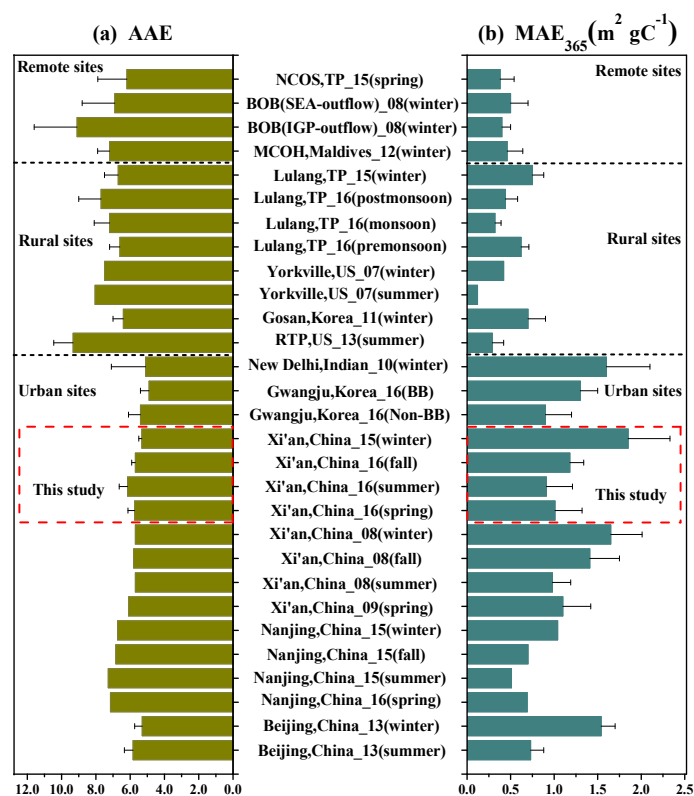
724 **Table 1.** Annual and seasonal mean contributions of measured PAHs, NACs and MOPs to  
 725 methanol-soluble BrC light absorption at 365 nm. Hyphens denote the measured value of more  
 726 than one third of the samples is below the detection limit.

Compounds	MAE <sub>365</sub> (m <sup>2</sup> gC <sup>-1</sup> )	Contribution to BrC light absorption at 365 nm (%)				
		Annual	Spring	Summer	Fall	Winter
Fluoranthene (FLU)	4.25	0.11	0.05	0.02	0.05	0.15
Pyrene (PYR)	0.46	0.01	0.00	0.00	0.01	0.01
Chrysene (CHR)	0.00	0.00	0.00	0.00	0.00	0.00
Benzo(a)anthracene (BaA)	2.06	0.04	0.01	0.01	0.02	0.05
Benzo(a)pyrene (BaP)	9.31	1.04	0.76	0.39	1.16	1.10
Benzo(b)fluoranthene (BbF)	4.10	0.17	0.14	0.07	0.17	0.18
Benzo(k)fluoranthene (BkF)	3.47	0.04	0.03	0.02	0.04	0.04
Indeno[1,2,3-cd]pyrene (IcdP)	4.68	0.51	0.50	0.24	0.71	0.46
Benzo(ghi)perylene (BghiP)	8.95	0.29	0.28	0.16	0.41	0.26
9,10-Anthracenequinone (9,10AQ)	0.28	0.01	0.00	0.00	0.00	0.01
Benzanthrone (BEN)	6.13	0.11	0.08	0.05	0.11	0.12
Benzo[b]fluoren-11-one (BbF11O)	1.89	0.02	0.02	0.01	0.02	0.03
4-Nitrophenol (4NP)	2.17	0.08	0.06	0.02	0.05	0.10
4-Nitro-1-naphthol (4N1N)	9.71	-	-	-	-	0.03
2-Methyl-4-nitrophenol (2M4NP)	2.81	0.03	0.01	0.01	0.01	0.04
3-Methyl-4-nitrophenol (3M4NP)	2.65	0.02	0.01	0.00	0.01	0.03
2,6-Dimethyl-4-nitrophenol (2,6DM4NP)	3.27	-	-	-	-	0.01
4-Nitrocatechol (4NC)	7.91	0.27	0.05	0.03	0.20	0.35
3-Methyl-5-nitrocatechol (3M5NC)	5.77	-	-	-	0.05	0.11
4-Methyl-5-nitrocatechol (4M5NC)	7.29	-	-	-	0.06	0.13
3-Nitrosalicylicacid (3NSA)	3.86	-	-	-	-	0.01
5-Nitrosalicylicacid (5NSA)	3.36	0.03	0.01	0.02	0.04	0.02
Syringyl acetone (SyA)	0.25	0.01	0.01	0.00	0.01	0.01
Vanillin (VAN)	8.17	0.01	0.00	0.00	0.00	0.01
Vanillic acid (VaA)	0.66	0.00	0.00	0.00	0.00	0.00
Total	103.46	2.80	2.02	1.05	3.13	3.26

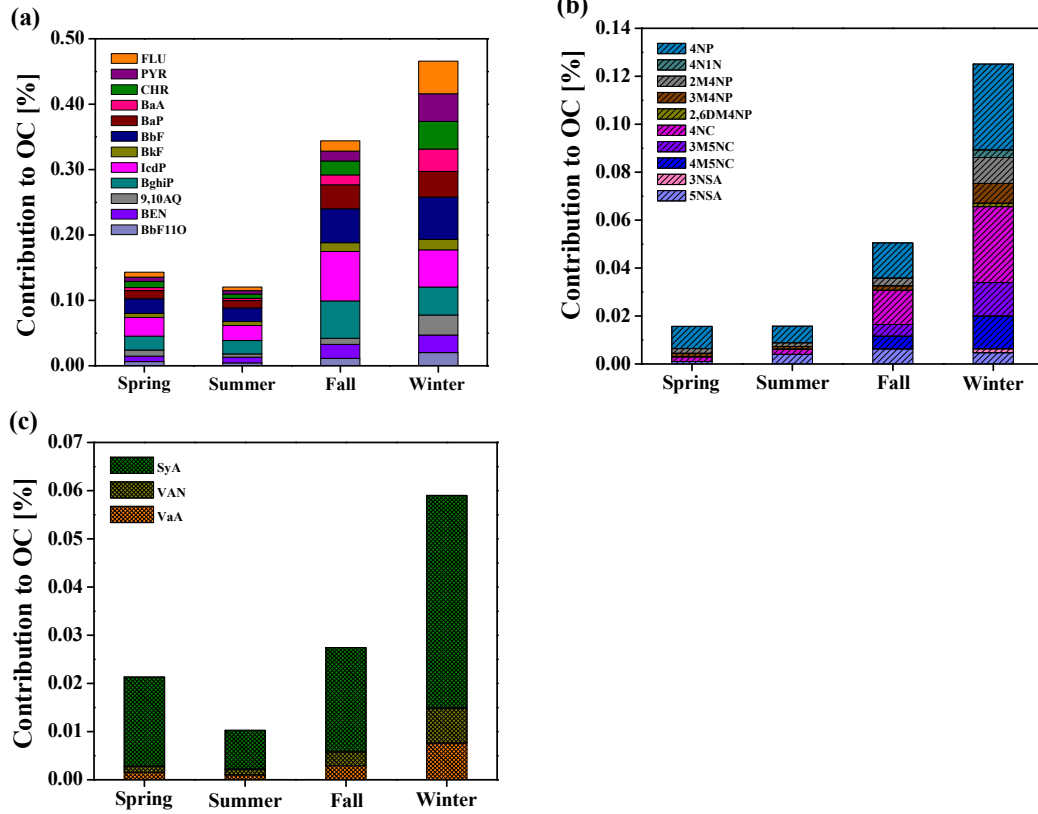


727

728 **Figure 1.** Time series of the light absorption coefficient of water-soluble and methanol-soluble  
 729 BrC at 365 nm ( $Abs_{365,WSOC}$  and  $Abs_{365,MSOC}$ , respectively), as well as OC and WSOC  
 730 concentrations.



731 **Figure 2.** Comparison of AAE (left column) and MAE<sub>365</sub> (right column) values of water-soluble  
 732 BrC at remote sites (Srinivas and Sarin, 2013; Bosch et al., 2014; Zhang et al., 2017b), rural  
 733 sites (Hocobian et al., 2010; Kirillova et al., 2014a; Zhu et al., 2018; Xie et al., 2019) and urban  
 734 sites (Kirillova et al., 2014b; Yan et al., 2015; Chen et al., 2018; Huang et al., 2018; Park et al.,  
 735 2018).

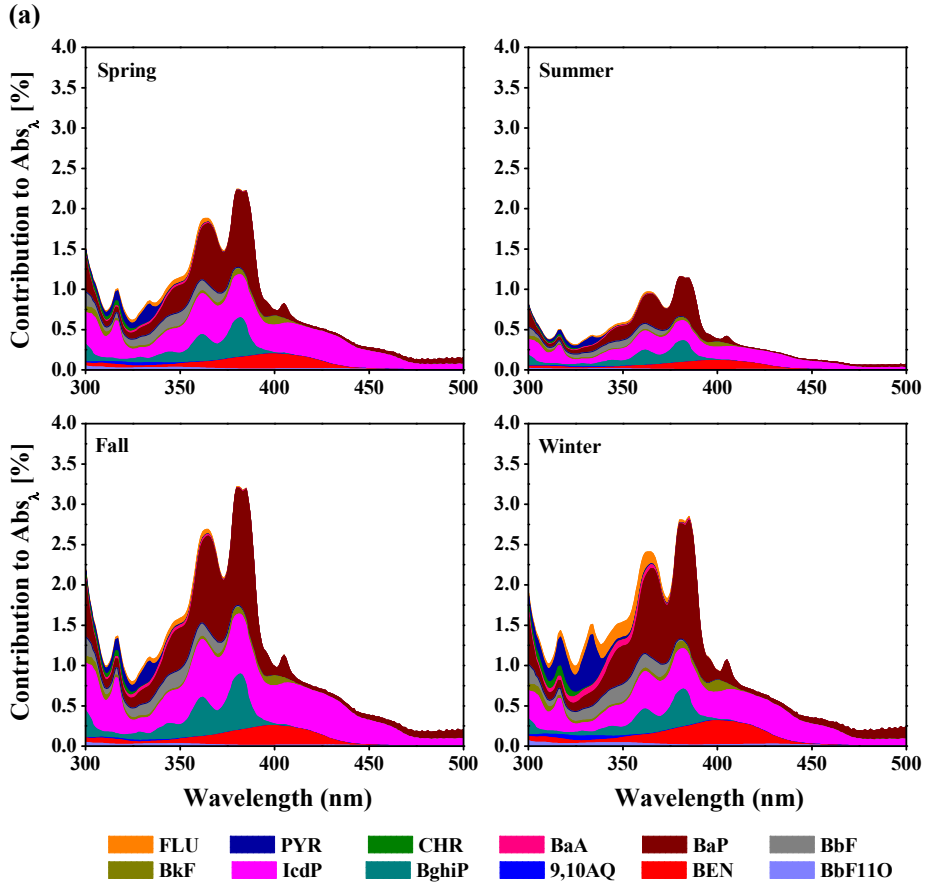


736

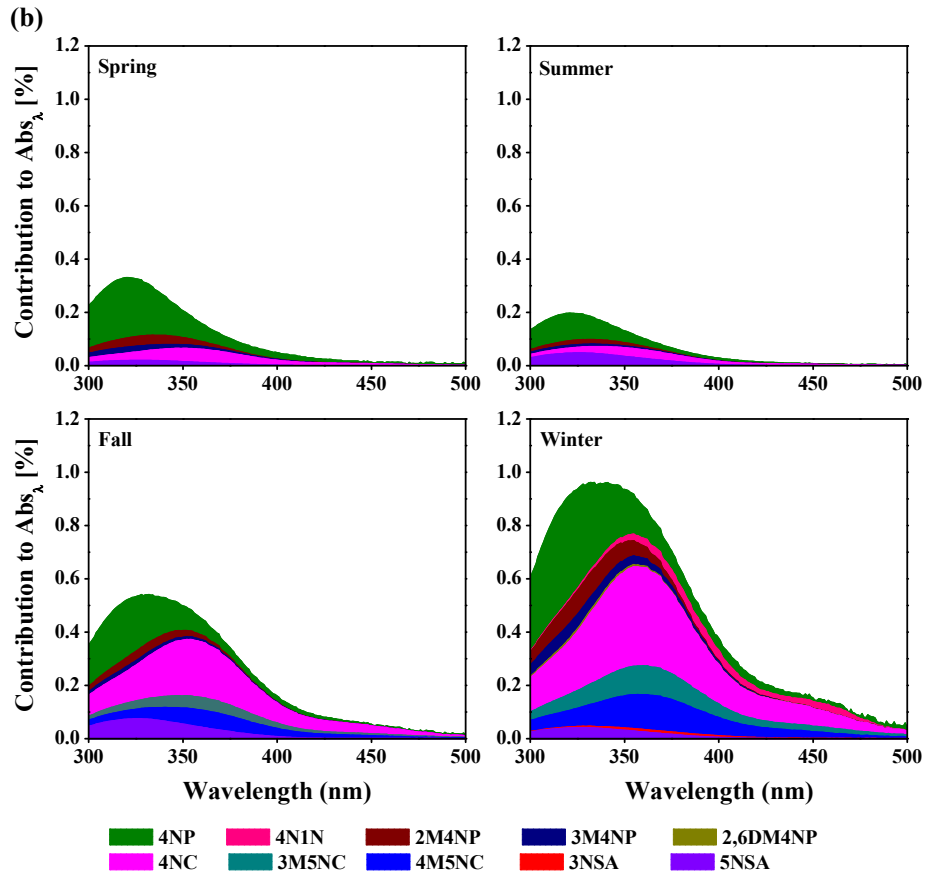
737  
738

739 **Figure 3.** Contributions of (a) PAHs, (b) NACs, and (c) MOPs carbon mass concentrations to  
740 the total OC concentrations.

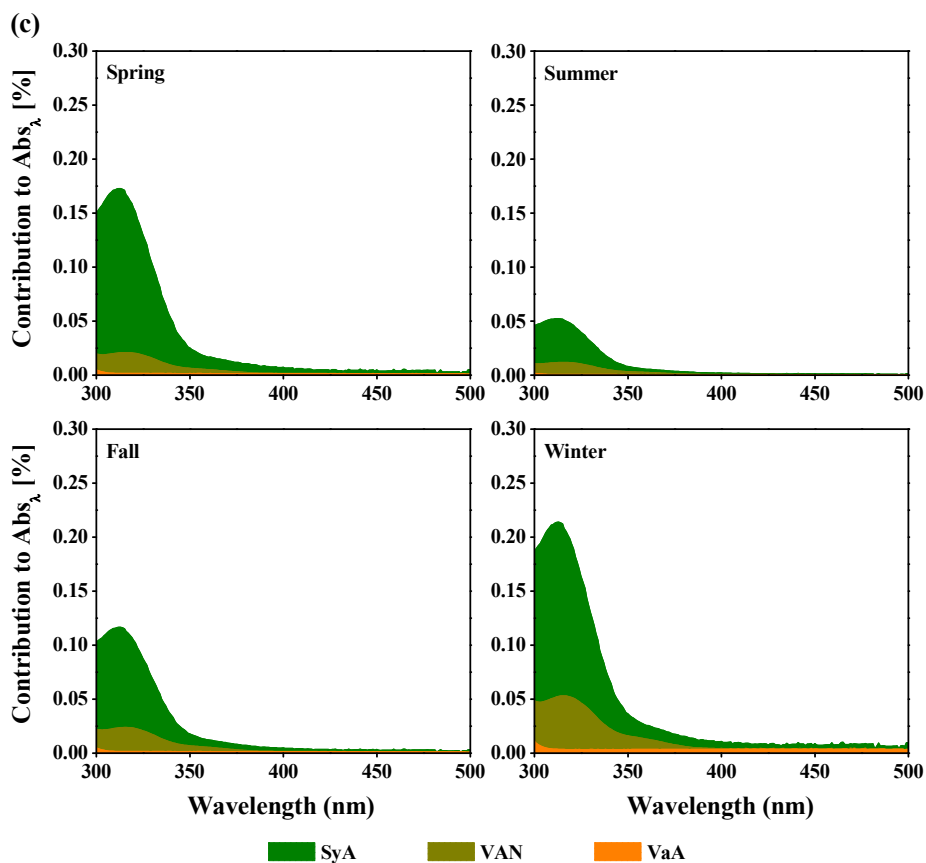
741



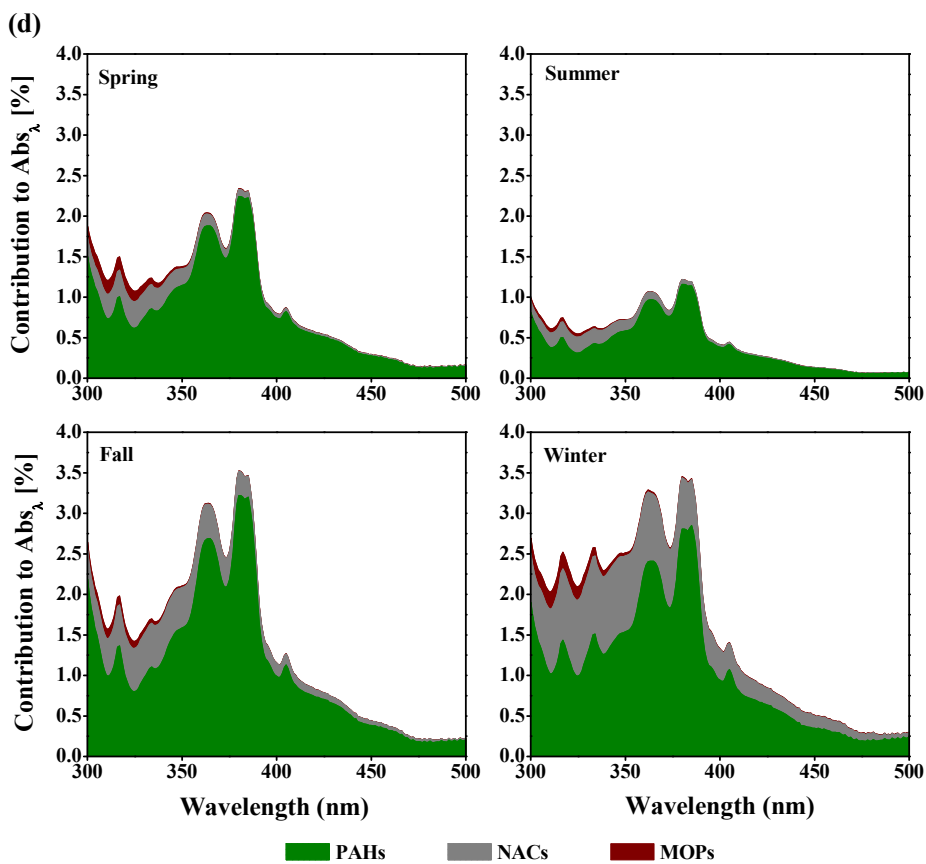
742



743



744

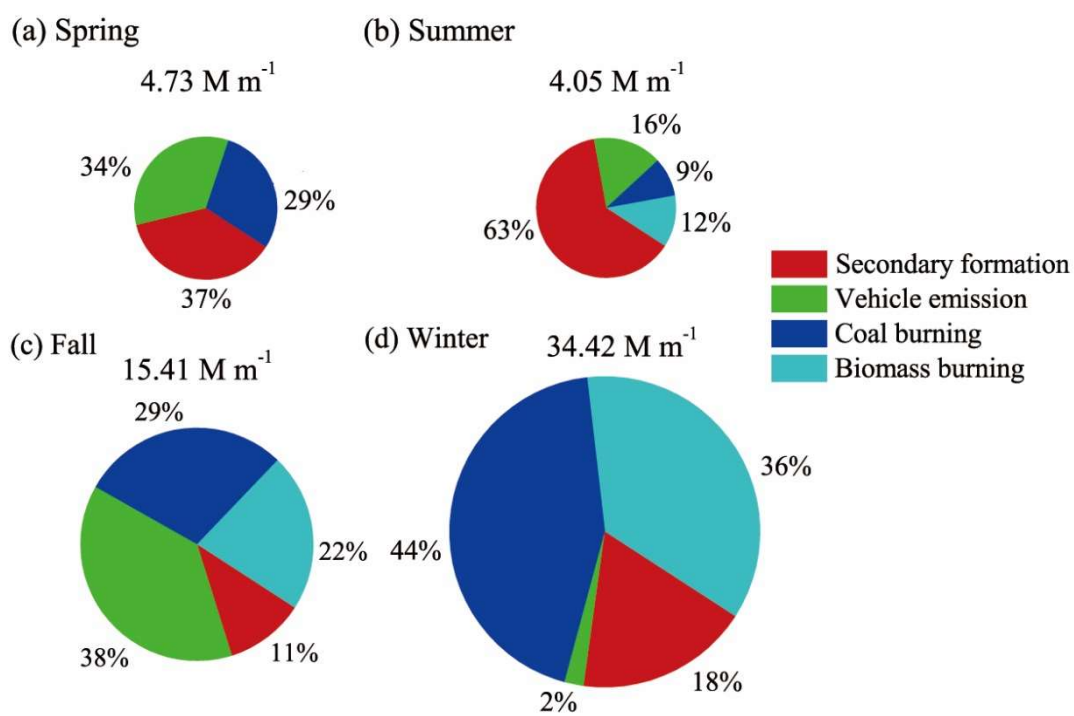


745

746 **Figure 4.** Light absorption contributions of (a) PAHs, (b) NACs, (c) MOPs and (d) total



747 measured chromophores to  $Abs_{MSOC}$  over the wavelength range of 300 to 500 nm in spring,  
748 summer, fall and winter.  
749



750

751 **Figure 5.** Contributions of the major sources to Abs<sub>365,MSOC</sub> in Xi'an during spring, summer, fall  
 752 and winter.